JBIC Journal of Biological Inorganic Chemistry (2019) 24:247–255
https://doi.org/10.1007/s00775-019-01642-9

ORIGINAL PAPER

Fluoride and azide binding to ferric human hemoglobin:haptoglobin complexes highlights the ligand-dependent inequivalence of the α and β hemoglobin chains

Paolo Ascenzi[1] · Alessandra di Masi[2] · Giovanna De Simone[2] · Magda Gioia[3,4] · Massimo Coletta[3,4]

Received: 18 October 2018 / Accepted: 31 December 2018 / Published online: 31 January 2019

Abstract

Haptoglobin (Hp) binds human hemoglobin (Hb), contributing to prevent extra-erythrocytic Hb-induced damage. Hp forms preferentially complexes with αβ dimers, displaying heme-based reactivity. Here, kinetics and thermodynamics of fluoride and azide binding to ferric human Hb (Hb(III)) complexed with the human Hp phenotypes 1-1 and 2-2 (Hp1-1:Hb(III) and Hp2-2:Hb(III), respectively) are reported (pH 7.0 and 20.0 °C). Fluoride binds to Hp1-1:Hb(III) and Hp2-2:Hb(III) with a one-step kinetic and equilibrium behavior. In contrast, kinetics of azide binding to and dissociation from Hp1-1:Hb(III)($-N_3^-$) and Hp2-2:Hb(III)($-N_3^-$) follow a two-step process. However, azide binding to Hp1-1:Hb(III) and Hp2-2:Hb(III) is characterized by a simple equilibrium, reflecting the compensation of kinetic parameters. The fast and the slow step of azide binding to Hp1-1:Hb(III) and Hp2-2:Hb(III) should reflect azide binding to the ferric β and α chains, respectively, as also proposed for the similar behavior observed in Hb(III). Present results highlight the ligand-dependent kinetic inequivalence of Hb subunits in the ferric form, reflecting structural differences between the two subunits in the interaction with some ferric ligands.

Graphical abstract

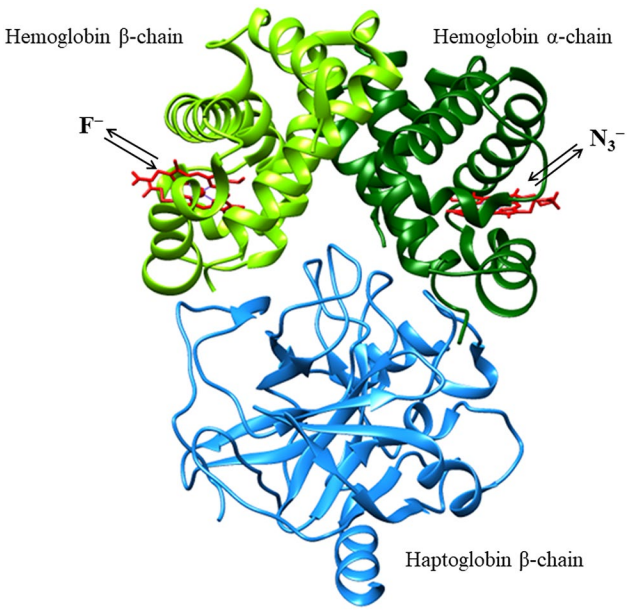

Keywords Human haptoglobin 1-1:hemoglobin complex · Human haptoglobin 2-2:hemoglobin complex · Azide binding · Fluoride binding · Kinetics · Thermodynamics

Extended author information available on the last page of the article

Abbreviations

CCP domain	Complement control protein domain
Hb	Human hemoglobin
Hb(III)	Ferric Hb
Hp	Human haptoglobin
Hp1-1	Phenotype 1-1 of Hp
Hp2-2	Phenotype 2-2 of Hp
Hp1-1:Hb(III)	Ferric Hp1-1:Hb complex
Hp2-2:Hb(III)	Ferric Hp 2-2:Hb complex
SP-like domain	Serine protease-like domain

Introduction

The release of hemoglobin (Hb) into plasma occurs physiologically during the hemolysis of senescent erythrocytes and the enucleation of erythroblasts, or as the consequence of severe hematologic diseases and blood transfusion [1–4]. As high levels of free Hb in plasma can catalyze the formation of free radicals and mediate the destruction of cellular constituents and extracellular macromolecules, biological systems require an efficient mechanism for Hb scavenging [5–7]. The molecular chaperone haptoglobin (Hp) binds free plasma Hb leading to a very stable non-covalent complex. This allows Hb clearance via the reticuloendothelial system and the CD163 receptor-mediated endocytosis in hepatocytes, Kupffer cells, and tissue macrophages [4, 8–11].

Human Hp is a 90-kDa protein encoded by two different alleles (i.e., Hp1 and Hp2) of the *HP* gene. The occurrence of the Hp1 and Hp2 alleles in humans gives rise to Hp1-1 dimers (linked by the Cys15–Cys15 bridge), Hp1-2 hetero-oligomers and Hp2-2 oligomers (linked by the Cys15–Cys15 and Cys74–Cys74 bridges) [12]. The most abundant oligomer of Hp2-2 is the tetramer, but trimers and higher order oligomers have been recently observed [11–14]. Hp is a single polypeptide chain made up of two α and one β domains; it is organized in a serine protease-like (SP-like) domain and two complement control protein (CCP) domains [11, 12, 15–17]. The SP-like domain of Hp forms tight extensive interactions with both the α- and β-subunits of Hb, interfering with the Hb αβ dimer–dimer interface of the native Hb tetramer, thus stabilizing the $\alpha_1\beta_1$ dimer [18] and impairing the heme oxidation and release. Moreover, the burying of several Hb residues in the Hp:Hb interface shields them from oxidative modification [13, 14].

Ferric and ferrous Hp:Hb complexes display functional properties that are reminiscent of those of the Hb R-state, as expected for the αβ dimers of Hb. In fact, the Hp:Hb complexes display a high ligand affinity and reactivity, no "heme–heme interactions", and no Bohr effect [11, 13, 14, 19–28]. Moreover, two equimolar redox systems are present in the Hpl-l:Hb and Hp2-2:Hb complexes reflecting the redox potential of the α and β chains (~0.05 V and 0.11 V, respectively), which are in good agreement with the results on tetrameric Hb and the isolated Hb chains [21].

Since ligand binding to ferric Hb has been reported to display different behaviors [22, 29], we decided to investigate in detail the reaction of fluoride and azide with ferric human Hb complexed with the human Hp1-1 and Hp2-2 (Hp1-1:Hb(III) and Hp2-2:Hb(III), respectively). The relevance of this study resides on the fact that upon binding Hp tetrameric Hb(III) dissociates completely in the $\alpha_1\beta_1$ (as well as $\alpha_2\beta_2$) dimers, destroying the $\alpha_1\beta_2$ (as well as the $\alpha_2\beta_1$) interactions, which are responsible for most of the cooperativity present in the tetrameric assembly [30]. Moreover, this investigation represents a unique opportunity to study functional properties of the dimeric assembly without the interference of the tetrameric population, always present to a relevant extent even at the lowest affordable concentrations (i.e., 0.5–1.0 μM) [31]. Kinetics and thermodynamics of fluoride binding to Hp1-1:Hb(III) and Hp2-2:Hb(III) are strictly monophasic. However, kinetics of azide binding and dissociation follow a two-step process, even though azide-binding equilibrium curve is characterized by a simple hyperbola; it likely reflects the compensation between association and dissociation kinetic parameters. Present results highlight the ligand-dependent kinetic inequivalence of Hb subunits in the ferric form, reflecting structural differences between the two subunits in the interaction with some ferric ligands.

Materials

Human Hp1-1 and Hp2-2 were obtained from Athens Research & Technology, Inc. (Athens, GA, USA). Human oxygenated Hb was prepared as previously reported [24]. The oxygenated Hp:Hb complexes were prepared by mixing oxygenated Hb with Hp1-1 and Hp2-2 at pH 7.0 and 20.0 °C, according to literature [21]. The dimeric Hp:tetrameric Hb stoichiometry was 1:1. To avoid the occurrence of free Hb, a 20% excess of Hp1-1 and Hp2-2 was present in all samples and the absence of free Hb was checked by gel electrophoresis [21]. Hp1-1:Hb(III) and Hp2-2:Hb(III) were prepared by adding few grains of ferricyanide to the oxygenated Hp:Hb solutions [32, 33]. All the other chemicals were purchased from Merck AG (Darmstadt, Germany) and Sigma-Aldrich (St. Louis, MO, USA). All chemicals were of analytical grade and were used without further purification.

Methods

Fluoride binding to Hp1-1:Hb(III) and Hp2-2:Hb(III) was analyzed in the framework of Scheme 1:

$$\mathrm{Hp{:}Hb(III)} + \mathrm{F^-} \underset{k_{off}}{\overset{k_{on}}{\rightleftarrows}} \mathrm{Hp{:}Hb(III){-}F^-}$$

Scheme 1 Fluoride binding to Hp1-1:Hb(III) and Hp2-2:Hb(III)

$$\mathrm{Hp{:}Hb(III)} + \mathrm{N_3^-} \underset{k_{off}}{\overset{k_{on}}{\rightleftarrows}} \mathrm{Hp{:}Hb(III){-}N_3^-}$$

Scheme 2 Azide binding to Hp1-1:Hb(III) and Hp2-2:Hb(III)

Values of the apparent first-order rate constants for fluoride binding to Hp1-1:Hb(III) and Hp2-2:Hb(III) (i.e., k) were obtained by rapid mixing the Hp1-1:Hb(III) and Hp2-2:Hb(III) solutions (final concentration, 4.8×10^{-6} M to 5.3×10^{-6} M) with the fluoride solution (final concentration, 1.0×10^{-3} M to 1.0 M).

Values of k were obtained according to the following equations:

$$\left[\mathrm{Hp{:}Hb(III)}\right]_t = \left[\mathrm{Hp{:}Hb(III)}\right]_i \times \mathrm{e}^{-k\times t}, \tag{1}$$

$$\left[\mathrm{Hp{:}Hb(III)}\right]_t = \left[\mathrm{Hp{:}Hb(III)}\right]_i \times (1-\mathrm{e}^{-k\times t}), \tag{2}$$

depending on the observation wavelength. Hp:Hb(III) indicates either Hp1-1:Hb(III) or Hp2-2:Hb(III). The amplitude of the time courses was normalized to that observed at 410 nm.

Values of the apparent second-order rate constant for fluoride binding to Hp1-1:Hb(III) and Hp2-2:Hb(III) (i.e., k_{on}; Scheme 1) and of apparent first-order rate constant for fluoride dissociation from Hp1-1:Hb(III)-F^- and Hp2-2:Hb(III)-F^- (i.e., k_{off}; Scheme 1) were obtained according to the following equation:

$$k = k_{on} \times [\mathrm{F^-}] + k_{off}. \tag{3}$$

Values of the apparent dissociation equilibrium constant for fluoride binding to Hp1-1:Hb(III) and Hp2-2:Hb(III) (i.e., $K = k_{off}/k_{on}$; Scheme 1) were determined from the dependence of the molar fraction of fluoride-bound Hp1-1:Hb(III) and Hp2-2:Hb(III) (i.e., Y) on the ligand concentration (i.e., [F^-]) according to the following equation:

$$Y = [\mathrm{F^-}]^n/([\mathrm{F^-}]^n + K^n), \tag{4}$$

where n is the Hill coefficient.

Azide binding to Hp1-1:Hb(III) and Hp2-2:Hb(III) was analyzed in the framework of Scheme 2.

Azide binding to Hp1-1:Hb(III) and Hp2-2:Hb(III) has been investigated by rapid mixing the Hp1-1:Hb(III) and Hp2-2:Hb(III) solutions (final concentration, 2.1×10^{-6} M to 2.5×10^{-6} M) with the azide solution (final concentration, 2.0×10^{-4} M to 5.0×10^{-3} M). Since for both Hp1-1:Hb(III) and Hp2-2:Hb(III) two exponentials were observed, values of the two first-order rate constants (i.e., k_1 and k_2) were obtained according to the following equations [22]:

$$\begin{aligned}\left[\mathrm{Hp{:}Hb(III)}\right]_t = {} & a\times\left[\mathrm{Hp{:}Hb(III)}\right]_i \times \mathrm{e}^{-k1\times t} \\ & + b\times\left[\mathrm{Hp{:}Hb(III)}\right]_i \times \mathrm{e}^{-k2\times t},\end{aligned} \tag{5}$$

$$\begin{aligned}\left[\mathrm{Hp{:}Hb(III)}\right]_t = {} & a\times\left[\mathrm{Hp{:}Hb(III)}\right]_i \times (1-\mathrm{e}^{-k1\times t}) \\ & + b\times\left[\mathrm{Hp{:}Hb(III)}\right]_i \times (1-\mathrm{e}^{-k2\times t}),\end{aligned} \tag{6}$$

depending on the observation wavelength. Hp:Hb(III) indicates either Hp1-1:Hb(III) or Hp2-2:Hb(III), and a and b indicate the amplitude of the slow and fast binding processes, respectively, ($a+b=1$). The amplitude of the time courses was normalized to that observed at 420 nm.

Values of the apparent second-order rate constant for azide binding to Hp1-1:Hb(III) and Hp2-2:Hb(III) and of the apparent first-order rate constant for azide dissociation from Hp1-1:Hb(III)-N_3^- and Hp2-2:Hb(III)-N_3^- (i.e., k_{on1} and k_{off1}, and k_{on2} and k_{off2}, respectively; Scheme 2) were obtained according to Eq. 7:

$$k = k_{on} \times \left[\mathrm{N_3^-}\right] + k_{off}, \tag{7}$$

where k_{on} and k_{off} are either k_{on1} and k_{off1} or k_{on2} and k_{off2}.

The value of the apparent dissociation equilibrium constant for azide binding to Hp1-1:Hb(III) and Hp2-2:Hb(III) (*i.e.*, $K = k_{off}/k_{on}$; Scheme 2) was determined from the dependence of the molar fraction of azide-bound Hp1-1:Hb(III) and Hp2-2:Hb(III) (i.e., Y) on the ligand concentration (i.e., [N_3^-]) according to the following equation:

$$Y = \left[\mathrm{N_3^-}\right]^n/\left(\left[\mathrm{N_3^-}\right]^n + K^n\right), \tag{8}$$

where n is the Hill coefficient.

Azide and fluoride binding to Hp1-1:Hb(III) and Hp2-2:Hb(III) was investigated at pH 7.0 (5.0×10^{-2} phosphate buffer), at $T = 20.0$ °C. Azide and fluoride binding to Hp1-1:Hb(III) and Hp2-2:Hb(III) was monitored by single-wavelength stopped-flow spectroscopy between 380 and 460 nm. All kinetic experiments have been carried out with the BioLogic SFM-200 rapid-mixing stopped-flow apparatus (Claix, France); the dead-time of the stopped-flow apparatus was 1.4 ms and the observation chamber was 1 cm. All equilibria have been carried out with the Agilent 8453 UV–Vis spectroscopy system (Agilent Technologies Inc., Santa Clara, CA, USA). The results are given as mean values of at least four experiments plus or minus the corresponding standard deviation. All data were analyzed using the GraphPad Prism program, version 5.03 (GraphPad Software, La Jolla, CA, USA).

Results and discussion

Mixing the Hp1-1:Hb(III) and Hp2-2:Hb(III) solutions with the fluoride solution induces a shift of the optical absorption maximum and of the extinction coefficient of the Soret band (Table 1). The values of λ_{max} and ε of the absolute absorption spectra of Hp1-1:Hb(III), Hp2-2:Hb(III), Hp1-1:Hb(III)-F^-, and Hp2-2:Hb(III)-F^- match very well with those of mammalian ligand-free and ligand-bound Hb(III) and Mb(III) [24]. The kinetic and static difference absorbance spectra of Hp1-1:Hb(III) minus Hp1-1:Hb(III)-F^- (Fig. 1a) and Hp2-2:Hb(III) minus Hp2-2:Hb(III)-F^- (Fig. 1b) match very well each other.

Under all the experimental conditions, the time course for fluoride binding to Hp1-1:Hb(III) and Hp2-2:Hb(III) corresponds to a single exponential process for more than $96 \pm 5\%$ of its course (Scheme 1, Eqs. 1 and 2, and Fig. 1c, d). Values of the apparent pseudo-first-order rate constant for fluoride binding to Hp1-1:Hb(III) and Hp2-2:Hb(III) (i.e., k), determined according to Eqs. 1 and 2, depend linearly on the fluoride concentration (Fig. 1e, f). The analysis of data shown in Fig. 1e, f according to Eq. 3 allowed the determination of values of k_{on} (representing the slope of the straight lines) and of k_{off} (representing the intercept of the straight lines with the ordinate axis) (Table 2) for fluoride binding and dissociation, respectively (Table 2).

As shown in Fig. 1g, h, values of Y increase hyperbolically with the fluoride concentration tending to level off at $Y \gg K$ (see Scheme 1, and Eq. 4). The analysis of data shown in Fig. 1g, h according to Eq. 4 allowed the determination of values of K (Table 2). As expected for simple equilibria (i.e., data fitting with Eq. 4), values of the Hill coefficient n range between 0.99 ± 0.2 and 1.01 ± 0.2.

According to Scheme 1, values of k_{off}/k_{on} for fluoride binding to Hp1-1:Hb(III) and Hp2-2:Hb(III) (1.8×10^{-2} M and 1.6×10^{-2} M, respectively) are in excellent agreement with those of K ($= 1.6 \times 10^{-2}$ M and 1.9×10^{-2} M, respectively) (Table 2).

Table 1 Values of λ_{max} and ε of the absolute absorption spectra of ligand-free and ligand-bound Hp1-1:Hb(III) and Hp2-2:Hb(III)

Heme-protein	Ligand	λ_{max} (nm)	ε (M^{-1} cm^{-1})
Hp1-1:Hb(III)	–	406	171
Hp2-2:Hb(III)	–	405	173
Hp1-1:Hb(III)	Fluoride	402	148
Hp2-2:Hb(III)	Fluoride	402	146
Hp1-1:Hb(III)	Azide	418	137
Hp2-2:Hb(III)	Azide	402	136

pH 7.0 and 20.0 °C

Fig. 1 Fluoride binding to Hp1-1:Hb(III) and Hp2-2:Hb(III), at pH 7.0 and 20.0 °C. **a** Kinetic (squares) and static (circles) difference absorbance spectra of Hp1-1:Hb(III) minus Hp1-1:Hb(III)-F^-. **b** Kinetic (squares) and static (circles) difference absorbance spectra of Hp2-2:Hb(III) minus Hp2-2:Hb(III)-F^-. **c** Normalized averaged time courses of fluoride binding to Hp1-1:Hb(III). The fluoride concentration was 2.0×10^{-1} M (trace a), and 5.0×10^{-1} M (trace b). The time course analysis according to Eq. 1 allowed the determination of the following values of $k = 8.8 \times 10^{-1}$ s^{-1} (trace a) and $k = 2.2$ s^{-1} (trace b). **d** Normalized averaged time courses of fluoride binding to Hp2-2:Hb(III). The fluoride concentration was 2.0×10^{-1} M (trace a), and 5.0×10^{-1} M (trace b). The time course analysis according to Eq. 1 allowed the determination of the following values of $k = 9.5 \times 10^{-1}$ s^{-1} (trace a) and $k = 2.4$ s^{-1} (trace b). **e** Dependence of k on the ligand concentration for fluoride binding to Hp1-1:Hb(III). The analysis of data according to Eq. 3 allowed the determination of the following values of $k_{on} = 4.2 \pm 0.3$ M^{-1} s^{-1} and $k_{off} = (7.6 \pm 0.8) \times 10^{-2}$ s^{-1}. **f** Dependence of k on the ligand concentration for fluoride binding to Hp2-2:Hb(III). The analysis of data according to Eq. 3 allowed the determination of the following values of $k_{on} = 4.6 \pm 0.4$ M^{-1} s^{-1} and $k_{off} = (7.2 \pm 0.8) \times 10^{-2}$ s^{-1}. **g** Dependence of Y on the ligand concentration for fluoride binding to Hp1-1:Hb(III). The analysis of data according to Eq. 4 allowed the determination of the following value of $K = (1.6 \pm 0.2) \times 10^{-2}$ M. **h** Dependence of Y on the ligand concentration for fluoride binding to Hp2-2:Hb(III). The analysis of data according to Eq. 4 allowed the determination of the following value of $K = (1.9 \pm 0.2) \times 10^{-2}$ M. Where not shown, the error bars are smaller than the symbols

Mixing the Hp1-1:Hb(III) and Hp2-2:Hb(III) solutions with the azide solution induces a shift of the optical absorption maximum and of the extinction coefficient of the Soret band (Table 1). The values of λ_{max} and ε of the absolute absorption spectra of Hp1-1:Hb(III), Hp2-2:Hb(III), Hp1-1:Hb(III)-N_3^- and Hp2-2:Hb(III)-N_3^- match very well with those of mammalian ligand-free and ligand-bound Hb(III) and Mb(III) [24].

However, unlike for fluoride, kinetics of azide binding are biphasic and the relative amplitude of the absorbance changes is 0.48 ± 0.04 and 0.51 ± 0.05 over the whole wavelength range explored (i.e., between 380 nm and 460 nm). On the other hand, thermodynamics of azide binding to Hp1-1:Hb(III) and Hp2-2:Hb(III) follows a simple process. The kinetic and static difference absorbance spectra of Hp1-1:Hb(III) minus Hp1-1:Hb(III)-N_3^- (Fig. 2a) and Hp2-2:Hb(III) minus Hp2-2:Hb(III)-N_3^- (Fig. 2b) match very well each other.

Under all the experimental conditions, the time course for azide binding to Hp1-1:Hb(III) and Hp2-2:Hb(III) corresponds to a two-exponential process for more than $97 \pm 4\%$ of its course (Scheme 2, Eqs. 5 and 6, and Fig. 2c, d). Values of the apparent pseudo-first-order rate constants for azide binding to Hp1-1:Hb(III) and Hp2-2:Hb(III) (i.e., k_1 and k_2), determined according to Eq. 7, depend linearly on the azide concentration (Fig. 2e, f). The analysis of data shown in Fig. 1e, f according to Eq. 7 allowed the determination of values of k_{on1} and k_{on2} (representing the slope of the straight

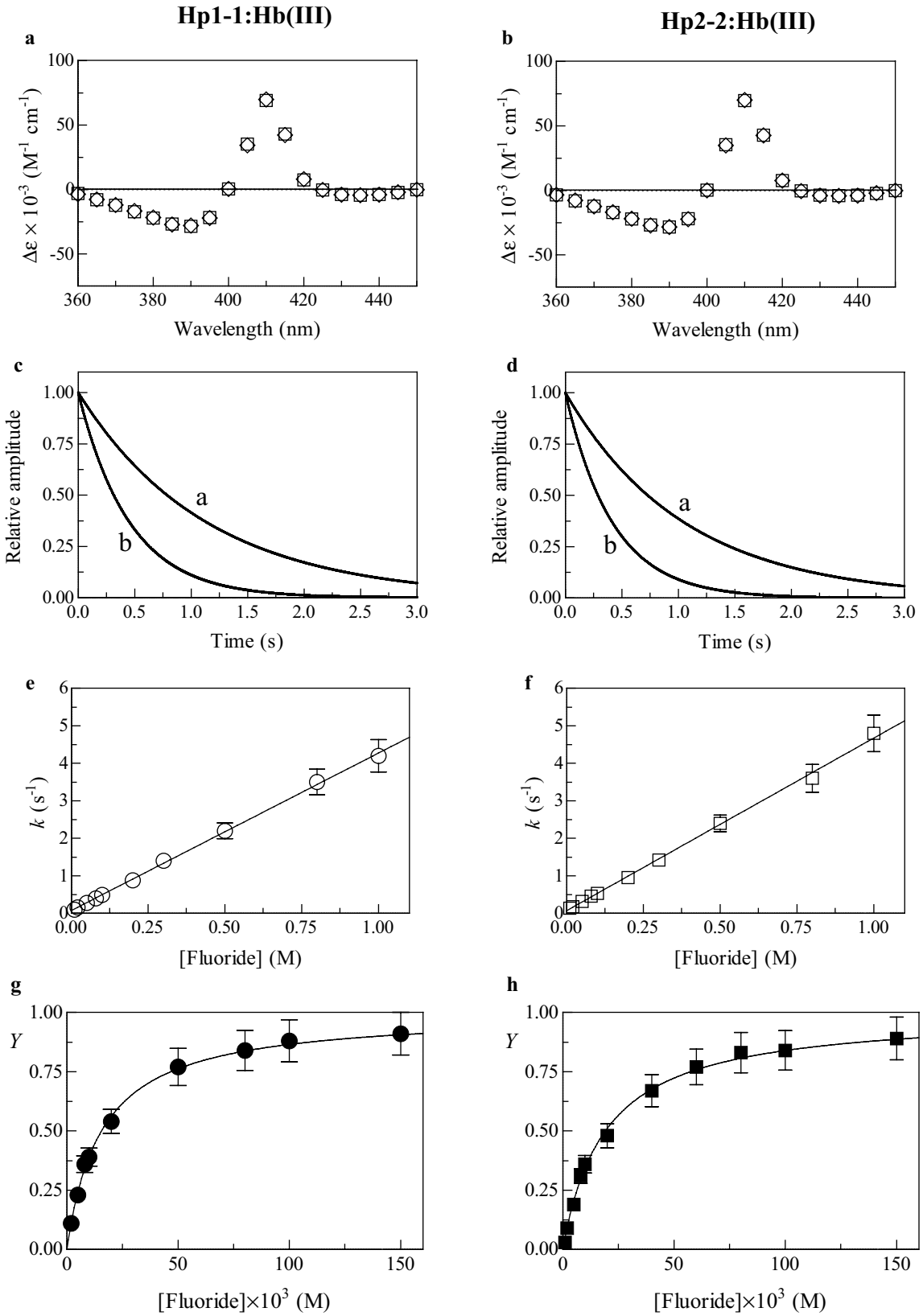
Hp1-1:Hb(III)
Hp2-2:Hb(III)
a
b
c
d
e
f
g
h
Δε × 10^-3 (M^-1 cm^-1)
Wavelength (nm)
Relative amplitude
Time (s)
k (s^-1)
[Fluoride] (M)
Y
[Fluoride]×10^3 (M)

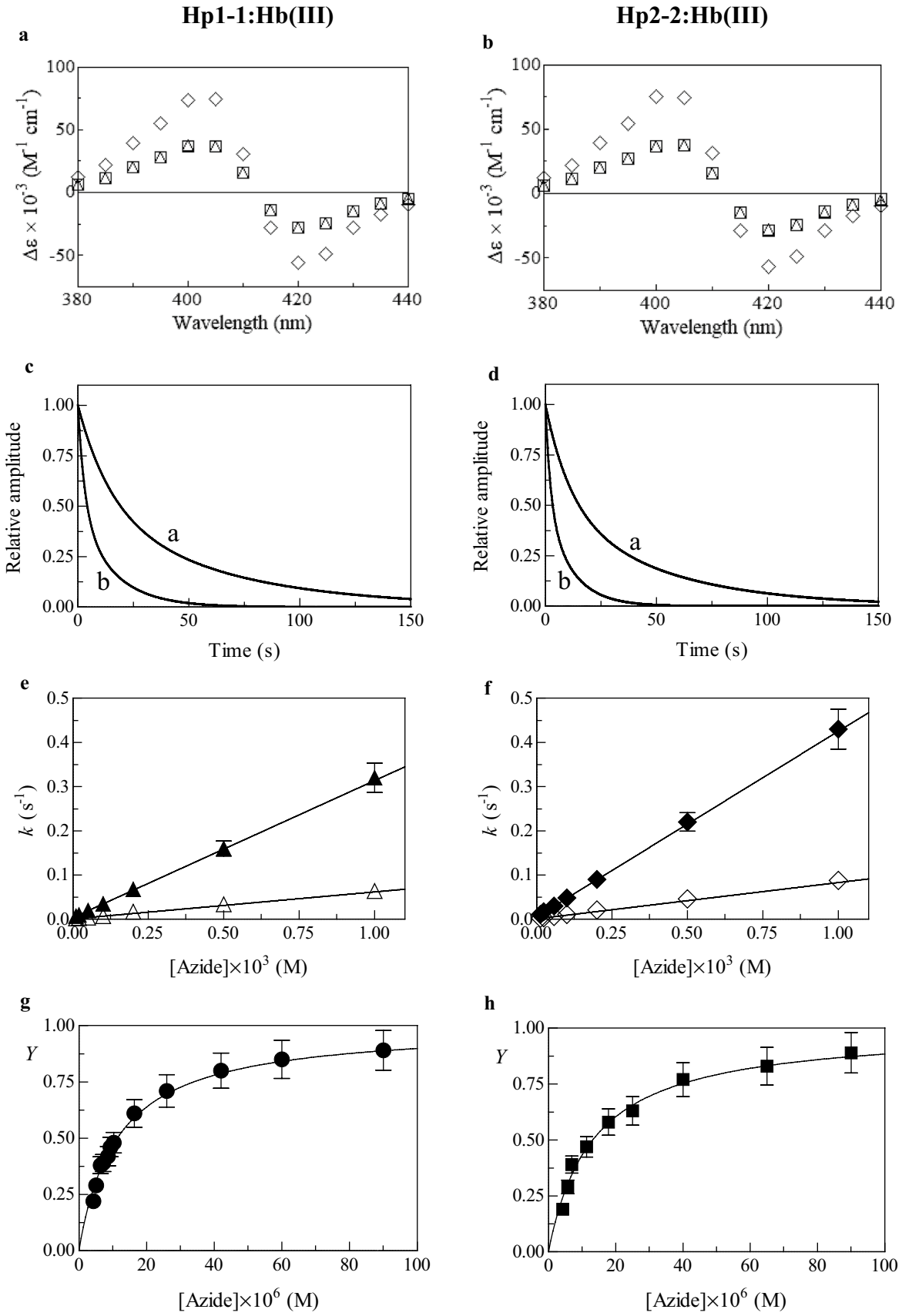
Hp1-1:Hb(III)
Hp2-2:Hb(III)
a
b
c
d
e
f
g
h
Δε × 10^-3 (M^-1 cm^-1)
Wavelength (nm)
Relative amplitude
Time (s)
k (s^-1)
[Azide]×10^3 (M)
Y
[Azide]×10^6 (M)

◂**Fig. 2** Azide binding to Hp1-1:Hb(III) and Hp2-2:Hb(III), at pH 7.0 and 20.0 °C. **a** Kinetic (squares and triangles) and static (diamonds) difference absorbance spectra of Hp1-1:Hb(III) minus Hp1-1:Hb(III)-N_3^-. **b** Kinetic (squares and triangles) and static (diamonds) difference absorbance spectra of Hp2-2:Hb(III) minus Hp2-2:Hb(III)-N_3^-. **c** Normalized averaged time courses of azide binding to Hp1-1:Hb(III). The azide concentration was 2.0×10^{-4} M (trace a) and 1.0×10^{-3} M (trace b). The time course analysis according to Eq. 5 allowed the determination of the following parameters: (trace a) $k_1=1.7\times10^{-2}$ s^{-1}, $a_1=0.51$, $k_2=6.8\times10^{-2}$ s^{-1}, and $a_2=0.49$; (trace b) $k_1=6.4\times10^{-2}$ s^{-1}, $a_1=0.48$, $k_2=3.2\times10^{-1}$ s^{-1}, and $a_2=0.52$. **d** Normalized averaged time courses of azide binding to Hp2-2:Hb(III). The azide concentration was 2.0×10^{-4} M (trace a), and 1.0×10^{-3} M (trace b). The time course analysis according to Eq. 5 allowed the determination of the following parameters: (trace a) $k_1=2.1\times10^{-2}$ s^{-1}, $a_1=0.52$, $k_2=9.0\times10^{-2}$ s^{-1}, and $a_2=0.48$; (trace b) $k_1=8.8\times10^{-2}$ s^{-1}, $a_1=0.51$, $k_2=4.3\times10^{-1}$ s^{-1}, and $a_2=0.49$. **e** Dependence of k_1 (filled triangles) and k_2 (open triangles) on the ligand concentration for azide binding to Hp1-1:Hb(III). The analysis of data according to Eq. 7 allowed the determination of the following parameters: (filled triangles) $k_{on1}=(3.1\pm0.3)\times10^{2}$ M^{1} s^{-1} and $k_{off1}=(3.7\pm0.5)\times10^{-3}$ s^{-1}; (open triangles) $k_{on2}=(6.1\pm0.6)\times10^{1}$ M^{1} s^{-1} and $k_{off2}=(8.0\pm1.0)\times10^{-4}$ s^{-1}. **f** Dependence of k_1 (filled diamonds) and k_2 (open diamonds) on the ligand concentration for azide binding to Hp2-2:Hb(III). The analysis of data according to Eq. 7 allowed the determination of the following parameters: (filled diamonds) $k_{on1}=(4.2\pm0.4)\times10^{2}$ M^{1} s^{-1} and $k_{off1}=(5.3\pm0.7)\times10^{-3}$ s^{-1}; (open diamonds) $k_{on2}=(8.2\pm0.8)\times10^{1}$ M^{1} s^{-1} and $k_{off2}=(1.0\pm0.2)\times10^{-3}$ s^{-1}. **g** Dependence of Y on the ligand concentration for azide binding to Hp1-1:Hb(III). The analysis of data according to Eq. 8 allowed the determination of the following value of $K=(1.1\pm0.1)\times10^{-5}$ M. **h** Dependence of Y on the ligand concentration for azide binding to Hp2-2:Hb(III). The analysis of data according to Eq. 8 allowed the determination of the following value of $K=(1.3\pm0.1)\times10^{-5}$ M. In the equilibrium experiments, the azide concentration refers to that of the free ligand. Where not shown, the error bars are smaller than the symbols

lines) and of k_{off1} and k_{off2} (representing the intercept of the straight lines with the ordinate axis) (Table 2).

As shown in Fig. 2g, h, values of Y increase hyperbolically with the azide concentration tending to level off at $Y \gg K$ (see Scheme 2, and Eq. 8). The analysis of data shown in Fig. 2g, h according to Eq. 8 allowed the determination of values of K (Table 2). As expected for simple equilibria (i.e., data fitting with Eq. 8), the values of the Hill coefficient n range between 0.98 ± 0.2 and 1.00 ± 0.2.

According to Scheme 1, values of k_{off1}/k_{on1} and k_{off2}/k_{on2} for azide binding to Hp1-1:Hb(III) and Hp2-2:Hb(III) (1.2×10^{-5} M and 1.4×10^{-5} M, and 1.3×10^{-5} M and 1.2×10^{-5} M, respectively) are in excellent agreement with those of K ($=1.1\times10^{-5}$ M and 1.3×10^{-5} M, respectively) (Table 2).

Fluoride binds to Hp1-1:Hb(III) and Hp2-2:Hb(III) with a one-step kinetic and equilibrium behavior as already reported for human Hb(III) [22]. The same behavior has been also reported for peroxynitrite scavenging [32, 34]. In contrast, kinetics of azide binding to Hp1-1:Hb(III) and Hp2-2:Hb(III) follows a two-step process, which is reminiscent to that reported for azide binding to tetrameric Hb(III), and isolated α(III) and β(III) chains. The heterogeneous azide-binding properties of tetrameric Hb(III) have been reported to reflect the different reactivity of α(III) and β(III) chains, as already reported by others [22, 29]. On this basis, the fast and the slow step of azide binding to Hp1-1:Hb(III) and Hp2-2:Hb(III) could reflect azide binding to the β(III) and α(III) chains, respectively (Table 2). However, azide binding to Hp1-1:Hb(III) and Hp2-2:Hb(III) at equilibrium is characterized by the compensation of kinetic parameters. In fact, values of k_{on1}/k_{on2} and of k_{off1}/k_{off2} for azide binding to Hp1-1:Hb(III) are 5.1 and 4.6, and values of k_{on1}/k_{on2} and of k_{off1}/k_{off2} for azide binding to Hp2-2:Hb(III) are 5.1 and 5.3. Consequently, the two-step kinetic behavior does not find a counterpart when ligand binding equilibria are investigated.

Present results open the question of the ligand-dependent kinetic inequivalence of Hb subunits in the ferric form. In fact, azide, nitrite, thiocyanide, and imidazole binding to Hb(III) is biphasic [22, 35], whereas fluoride, and cyanide recognition [22, 35] as well as peroxynitrite scavenging [34] is strictly monophasic.

The different behavior observed for fluoride and azide binding might find a structural basis on the evidence that upon fluoride association there is a contraction of the heme distal pocket closely similar for the two chains [36], whereas azide binding brings about an expansion of the heme distal pocket in β-chains and a slight contraction in α-subunits [37]. In particular, in β-chains the E helix moves away from the heme upon azide association relative to the ferric unbound Hb, expanding the ligand pocket; on the other hand, in α-chains the ligand pocket actually contracts slightly relative to ferric human Hb, as the E helix moves slightly towards the heme [37].

Concerning the behavior of the reduced form, it must be outlined that values of kinetic and/or thermodynamic parameters of ligand binding to Hp1-1:Hb(II) and Hp2-2:Hb(II) as well as of the (pseudo-)enzymatic properties of Hp:Hb(II) complexes match well with those of the Hb(II) R-state, which is typical of the αβ dimers of Hb(II) bound to Hp [20, 25, 27, 28, 32].

The different functional behavior between fluoride binding and azide binding to Hb(III) is mirrored in the case of the Hp1-1:Hb(III) and Hp2-2:Hb(III) complexes, displaying kinetic values closely similar (see Table 2). It may be worth underlining that these results represent the first direct and unequivocal evidence that the αβ dimers behave exactly as R-state tetramers; thus, only upon Hp binding all tetramers dissociate into the αβ dimers, giving rise to a homogeneous population and not a mixture of tetramers and dimers, as it occurs in dilute solutions of Hb(III) [31]. Therefore, the data shown in Table 2 represent a strong evidence that the dimeric Hp:Hb(III) complexes well represent the behavior

Table 2 Values of kinetic and thermodynamic parameters for fluoride and azide binding to and peroxynitrite detoxification from Hp1-1:Hb(III) and Hp2-2:Hb(III)

Heme-protein	Ligand	k_{on} (M^{-1} s^{-1})	k_{off} (s^{-1})	k_{off}/k_{on} (M)	K (M)
Hp1-1:Hb(III)[a]	Fluoride	4.2 ± 0.3	$(7.6 \pm 0.8) \times 10^{-2}$	1.8×10^{-2}	$(1.6 \pm 0.2) \times 10^{-2}$
Hp2-2:Hb(III)[a]	Fluoride	4.6 ± 0.6	$(7.2 \pm 0.8) \times 10^{-2}$	1.6×10^{-2}	$(1.9 \pm 0.2) \times 10^{-2}$
Hb(III)	Fluoride	4.0[b]			1.7×10^{-2}[c]

Heme-protein	Ligand	k_{on} (M^{-1} s^{-1})
Hp1-1:Hb(III)[d]	Peroxynitrite	1.7×10^{4}
Hp2-2:Hb(III)[d]	Peroxynitrite	1.6×10^{4}
Hb(III)[e]	Peroxynitrite	1.2×10^{4}

Heme-protein	Ligand	k_{on1} (M^{-1} s^{-1})	k_{on2} (M^{-1} s^{-1})	k_{off1} (s^{-1})	k_{off2} (s^{-1})	k_{off1}/k_{on1} (M)	k_{off2}/k_{on2} (M)	K (M)
Hp1-1:Hb(III)[a]	Azide	$(3.1 \pm 0.3) \times 10^{2}$	$(6.1 \pm 0.6) \times 10^{1}$	$(3.7 \pm 0.5) \times 10^{-3}$	$(8.0 \pm 0.1) \times 10^{-4}$	1.2×10^{-5}	1.4×10^{-5}	$(1.1 \pm 0.1) \times 10^{-5}$
Hp2-2:Hb(III)[a]	Azide	$(4.2 \pm 0.4) \times 10^{2}$	$(8.2 \pm 0.8) \times 10^{1}$	$(5.3 \pm 0.7) \times 10^{-3}$	$(1.0 \pm 0.2) \times 10^{-3}$	1.3×10^{-5}	1.2×10^{-5}	$(1.3 \pm 0.1) \times 10^{-5}$
Hb(III)	Azide	3.9×10^{2}[f]	6.9×10^{1}[f]	1.6×10^{-3}[f]	5.8×10^{-4}[f]	4.1×10^{-6}[f]	8.4×10^{-6}[f]	3.4×10^{-6}[g]
α chains Hb(III)	Azide	9.0×10^{1}[h]						1.2×10^{-5}[g]
β chains Hb(III)	Azide	4.0×10^{2}[h]						

[a]pH 7.0 and 20.0 °C. Present study
[b]pH 6.90 and 20.0 °C. From [22]
[c]pH 7.5 and 20.0 °C. From [39]
[d]pH 7.0 and 20.0 °C. From [33]
[e]pH 7.0 and 20.0 °C. From [34]
[f]pH 6.91 and 20.0 °C. From [22]
[g]pH 7.5 and 20.0 °C. From [40]
[h]pH 6.90 and 20.0 °C. From [22]

of R-state tetrameric Hb(III), indeed suggesting that in the $\alpha_1\beta_1$ (as well as in $\alpha_2\beta_2$) dimers the tertiary subunit structure and the inter-subunit interactions are closely similar to those observed in the R-state tetramer.

Finally, the exposure of the Hp:Hb complexes to hydrogen peroxide has been shown to induce the formation of ferryl metal centers, which are more kinetically inert than those of Hb. The stabilization of the Hb ferryl state by Hp plays a relevant role in the protection against Hb-mediated oxidative damage [38].

Acknowledgements The Grant of Dipartimenti di Eccellenza, MIUR (Legge 232/2016, Articolo 1, Comma 314-337) is gratefully acknowledged.

References

1. Muller-Eberhard U, Javid J, Liem HH, Hanstein A, Hanna M (1968) Blood 32:811–815
2. Bunn HF, Forget BG (1986) Hemoglobin: molecular, genetic and clinical aspects. Saunders, Philadelphia
3. Ascenzi P, Bocedi A, Visca P, Altruda F, Tolosano E, Beringhelli T, Fasano M (2005) IUBMB Life 57:749–759
4. Alayash AI, Andersen CB, Moestrup SK, Bülow L (2013) Trends Biotechnol 31:2–3
5. Alayash AI (2004) Nat Rev Drug Discov 3:152–159
6. Schaer DJ, Vinchi F, Ingoglia G, Tolosano E, Buehler PW (2014) Front Physiol 5:415
7. MacKellar M, Vigerust DJ (2016) Clin Diabetes 34:148–157
8. Kristiansen M, Graversen JH, Jacobsen C, Sonne O, Hoffman HJ, Law SK, Moestrup SK (2001) Nature 409:198–201
9. Buehler PW, Abraham B, Vallelian F, Linnemayr C, Pereira CP, Cipollo JF, Jia Y, Mikolajczyk M, Boretti FS, Schoedon G, Alayash AI, Schaer DJ (2009) Blood 113:2578–2586
10. Kaempfer T, Duerst E, Gehrig P, Roschitzki B, Rutishauser D, Grossmann J, Schoedon G, Vallelian F, Schaer DJ (2011) J Proteome Res 10:2397–2408
11. Andersen CBF, Stødkilde K, Sæderup KL, Kuhlee A, Raunser S, Graversen JH, Moestrup SK (2017) Antioxid Redox Signal 26:814–831
12. Polticelli F, Bocedi A, Minervini G, Ascenzi P (2008) FEBS J 275:5648–5656
13. Andersen CB, Torvund-Jensen M, Nielsen MJ, de Oliveira CL, Hersleth HP, Andersen NH, Pedersen JS, Andersen GR, Moestrup SK (2012) Nature 489:456–459
14. Stødkilde K, Torvund-Jensen M, Moestrup SK, Andersen CB (2014) Nat Commun 5:5487
15. Kurosky A, Barnett DR, Lee TH, Touchstone B, Hay RE, Arnott MS, Bowman BH, Fitch WM (1980) Proc Natl Acad Sci USA 77:3388–3392
16. Wejman JC, Hovsepian D, Wall JS, Hainfeld JF, Greer J (1984) J Mol Biol 174:319–341
17. Wejman JC, Hovsepian D, Wall JS, Hainfeld JF, Greer J (1984) J Mol Biol 174:343–368
18. Nagel RL, Gibson QH (1971) J Biol Chem 246:69–73
19. Nagel RL, Wittenberg JB, Ranney HM (1965) Biochim Biophys Acta 100:286–289

20. Nagel RL, Gibson QH (1966) J Mol Biol 22:249–255
21. Brunori M, Alfsen A, Saggese U, Antonini E, Wyman J (1968) J Biol Chem 243:2950–2954
22. Gibson QH, Parkhurst LJ, Geraci G (1969) J Biol Chem 244:4668–4676
23. Alfsen A, Chiancone E, Antonini E, Waks M, Wyman J (1970) Biochim Biophys Acta 207:395–403
24. Antonini E, Brunori M (1971) Hemoglobin and myoglobin in their reactions with ligands. North Holland Publishing Co, Amsterdam
25. Chiancone E, Antonini E, Brunori M, Alfsen A, Lavialle F (1973) Biochem J 133:205–207
26. Perutz MF (1979) Annu Rev Biochem 48:327–386
27. Azarov I, He X, Jeffers A, Basu S, Ucer B, Hantgan RR, Levy A, Kim-Shapiro DB (2008) Nitric Oxide 18:296–302
28. Ascenzi P, Tundo GR, Coletta M (2018) J Inorg Biochem 187:116–122
29. Coletta M, Angeletti M, De Sanctis G, Cerroni L, Giardina B, Amiconi G, Ascenzi P (1996) Eur J Biochem 235:49–53
30. Ackers GK, Doyle ML, Myers D, Daugherty MA (1992) Science 255:54–63
31. White SL (1975) J Biol Chem 250:1263–1268
32. Ascenzi P, De Simone G, Polticelli F, Gioia M, Coletta M (2018) J Biol Inorg Chem 23:437–445
33. Ascenzi P, Coletta M (2018) J Phys Chem B 122:11100–11107
34. Herold S, Shivashankar K (2003) Biochemistry 42:14036–14046
35. Klapper MH, Uchida H (1971) J Biol Chem 246:6849–6854
36. Deatherage JF, Loe RS, Moffat K (1976) J Mol Biol 104:723–728
37. Deatherage JF, Obendorf SK, Moffat K (1979) J Mol Biol 134:419–429
38. Banerjee S, Jia Y, Siburt CJ, Abraham B, Wood F, Bonaventura C, Henkens R, Crumbliss AL, Alayash AI (2012) Free Radic Biol Med 53:1317–1326
39. Anusiem AC, Beetlestone JG, Irvine DH (1968) J Chem Soc A 960–969
40. Bailey JE, Beetlestone JG, Irvine DH (1968) J Chem Soc A 2778–2783

Affiliations

Paolo Ascenzi[1] · Alessandra di Masi[2] · Giovanna De Simone[2] · Magda Gioia[3,4] · Massimo Coletta[3,4]

✉ Paolo Ascenzi
ascenzi@uniroma3.it

[1] Interdepartmental Laboratory for Electron Microscopy, Roma Tre University, Via della Vasca Navale 79, 00146 Roma, Italy

[2] Department of Sciences, Roma Tre University, Viale Marconi 446, 00146 Roma, Italy

[3] Department of Clinical Sciences and Translational Medicine, University of Roma "Tor Vergata", Via Montpellier 1, 00133 Roma, Italy

[4] Interuniversity Consortium for the Research on the Chemistry of Metals in Biological Systems, Via Celso Ulpiani 27, 70126 Bari, Italy